

***EXAMINATION OF MICROPHYSICAL RELATIONSHIPS AND  
CORRESPONDING MICROPHYSICAL PROCESSES IN WARM FOGS***

Chunsong Lu<sup>a, b</sup>, Yangang Liu<sup>b</sup>, Shengjie Niu<sup>a</sup>, Lijuan Zhao<sup>a</sup>

<sup>a</sup> School of Atmospheric Physics, Key Laboratory of Meteorological Disaster of Ministry of Education, Nanjing University of Information Science and Technology (NUIST), Jiangsu, China 210044

<sup>b</sup> Atmospheric Sciences Division, Brookhaven National Laboratory (BNL), Upton, NY 11973

Corresponding author: Chunsong Lu, Atmospheric Sciences Division, Brookhaven National Laboratory, Upton, NY 11973; Tel: 631-344-2458; Fax: 1-631-344-2887; luchunsong110@gmail.com

*Submitted to Atmospheric Environment*

October 2011

**Atmospheric Sciences Division/Environmental Sciences Dept.**

**Brookhaven National Laboratory**

**U.S. Department of Energy  
Office of Science**

Notice: This manuscript has been authored by employees of Brookhaven Science Associates, LLC under Contract No. DE-AC02-98CH10886 with the U.S. Department of Energy. The publisher by accepting the manuscript for publication acknowledges that the United States Government retains a non-exclusive, paid-up, irrevocable, world-wide license to publish or reproduce the published form of this manuscript, or allow others to do so, for United States Government purposes.

This preprint is intended for publication in a journal or proceedings. Since changes may be made before publication, it may not be cited or reproduced without the author's permission.

## **DISCLAIMER**

This report was prepared as an account of work sponsored by an agency of the United States Government. Neither the United States Government nor any agency thereof, nor any of their employees, nor any of their contractors, subcontractors, or their employees, makes any warranty, express or implied, or assumes any legal liability or responsibility for the accuracy, completeness, or any third party's use or the results of such use of any information, apparatus, product, or process disclosed, or represents that its use would not infringe privately owned rights. Reference herein to any specific commercial product, process, or service by trade name, trademark, manufacturer, or otherwise, does not necessarily constitute or imply its endorsement, recommendation, or favoring by the United States Government or any agency thereof or its contractors or subcontractors. The views and opinions of authors expressed herein do not necessarily state or reflect those of the United States Government or any agency thereof.

## **Abstract**

Microphysical relationships are examined for eight dense fog events from a comprehensive fog observation campaign carried out at Pancheng (32.2°N, 118.7°E) in the Nanjing area, China in the winter of 2007. Positive relationships are found among fog key microphysical properties (droplet number concentration, droplet size, spectral standard deviation, liquid water content) in every case. The responsible dominant processes are likely droplet nucleation with subsequent condensational growth and/or droplet deactivation via some complete droplet evaporation; turbulent and gravitational collision-coalescence processes also occur according to the abrupt spectral broadening, although not dominating. The combined effect of the dominant processes and collision-coalescence on microphysical relationships is further studied by dividing the dataset based on visibility or autoconversion threshold in every case. In different visibility or autoconversion threshold ranges, whether the number concentration is positively, negatively, or not related to the mean radius and spectral standard deviation depends on the competition between two processes (the compensation of small droplets due to nucleation and condensation and the loss of small droplets due to collision-coalescence); generally, positive relationships are found for different visibility or autoconversion threshold ranges in most cases, although negative relationships also appear sometimes when collision-coalescence is stronger with lower visibility or larger autoconversion threshold. Therefore, the compensation of small droplets is generally larger than the loss, which is greatly related to the sufficient fog condensation nuclei in this polluted area.

Keywords: warm fog; microphysical relationships; microphysical processes; observation

## 1. Introduction

Fog is a severe environmental hazard that greatly influences traffic, human health, and agricultural products, resulting in heavy economic losses (Gultepe et al., 2007; Haeffelin et al., 2010; Niu et al., 2010a). To reduce the losses, accurate fog forecast is necessary, and numerical forecast has attracted great efforts (Kong, 2002; Bergot et al., 2005; Fu et al., 2006, 2008; Gao et al., 2007; Rémy and Bergot, 2010; Shi et al., 2010, 2011; Yang et al., 2010; Zhou and Du, 2010; Kim, 2011; Porson et al., 2011; Stolaki et al., 2011; Thoma et al., 2011; Zhou et al., 2011). Whether the numerical forecast is accurate or not greatly depends on the parameterization of complicated physical processes in fog events (Croft et al., 1997; Gultepe et al., 2007). To explore the macro and micro physical processes, it is important to detect fog/cloud microphysical properties because different macro and micro processes affect fog/cloud size distributions and hence key microphysical properties (Liu et al., 2008). Furthermore, microphysical properties affect visibility, an important factor in fog forecast. Many researches related visibility to liquid water content (LWC) (e.g., Eldridge, 1971; Tomasi and Tampieri, 1976; Pinnick et al., 1978; Kunkel, 1984; Bergot and Guedalia, 1994; Stoelinga and Warner, 1999); more recently, Gultepe and Milbrandt (2007) extended the parameterization and related visibility to both LWC and droplet number concentration ( $N$ ). Therefore, studying on fog microphysics is necessary and important to improve fog forecast and reduce losses due to fog disasters.

In the past several decades, great efforts have been devoted to in situ observational study on fog microphysics (Eldridge, 1961; Pilié et al., 1975; Roach et al., 1976; Justo and Lala, 1980; Kunkel, 1984; Meyer et al., 1986; Gerber, 1991; Fuzzi et al., 1992; Wendisch et al., 1998; Gultepe and Milbrandt, 2007; Lu and Niu, 2008; Haeffelin et al., 2010; Niu et al., 2010b; Price, 2011). In most fog cases, LWC is lower than  $0.5 \text{ g m}^{-3}$  (e.g., Wobrock et al., 1992; Niu et al., 2010c);  $N$  is from a few tens to several hundreds  $\text{cm}^{-3}$  (e.g., García-García and Montañez, 1991; Klemm and Wrzesinsky, 2007; Gultepe et al., 2009), but  $N$  larger than  $1000 \text{ cm}^{-3}$  is also found in some polluted areas (e.g., Li, 2001; He et al., 2003; Niu et al., 2010c); both unimodal (e.g., García-García and Montañez, 1991; Li, 2001; Niu et al., 2010b; Gonser et al., 2011) and bimodal size distributions (e.g., Hong and Huang, 1965; Pilié et al., 1975; Roach et al., 1976; Meyer et al., 1980; Gerber, 1991; Wendisch et al., 1998; Huang et

al., 2000; Gultepe et al., 2009; Niu et al., 2011) have been observed in different fog cases. Furthermore, during one specific fog event, remarkable spatial and temporal variations of microphysical properties have been widely reported. Spatially, similar to inhomogeneity in clouds (e.g., Baumgardner et al., 1993; Burnet and Brenguier, 2007; Haman et al., 2007), García-García (2002) found inhomogeneous fog microphysical structure at a fine scale (less than 1 m). Temporally, microphysical properties varied evidently during a fog lifecycle; quasi-periodic oscillations of the microphysical properties and other related meteorological elements (e.g., temperature, wind speed) have been observed and simulated; different mechanisms for the quasi-periodic oscillations were proposed by different scholars, such as a cycle of fog dissipation and redevelopment processes associated with radiative cooling and turbulence (Welch et al., 1986), interaction between radiatively-induced droplet growth and subsequent depletion of droplets due to gravitational settling (Bott et al., 1990; Huang et al., 2000), advection of fog inhomogeneous spatial structure (Roach et al., 1976), and effect of gravity wave (Roach, 1976; Duynkerke, 1991).

Although the importance of fog microphysics and related processes has been recognized and considerable progress has been made, much remains elusive. For example, it is still unclear, in determining fog spectral shape, what the relationships among the effects of different factors and processes are and which one is the main process. Therefore, more state-of-the-art observations should be carried out, especially in China where past observations were largely based on gelatin-slide impactor systems with low sampling rate (Niu et al., 2010c).

A droplet spectrometer (FM-100; Droplet Measurement Technologies, Colorado, USA) with a sampling rate of 1 Hz was deployed in observations carried out at Pancheng (32°12'N, 118°42'E), Nanjing, China in every winter during 2006 - 2009. The data from this spectrometer provides a great opportunity to examine fog microphysics and the corresponding physical processes. Furthermore, Nanjing is a megacity in the Yangtze River Delta of China with high population density and a well-developed economy; urbanization has brought great stress to the local environment and emissions of pollutants (SO<sub>2</sub>, NO<sub>x</sub> and NH<sub>3</sub>) are one or two orders of magnitude higher than in Europe and South America (Lu et al., 2010a). Fog occurring in such an environment is expected to show unique

microphysical characteristics, compared with the fogs in clean areas. Using the in situ observation at Pancheng, Niu et al.(2010b) examined the main and minor processes in a dense fog in 2006 through analyzing the relationships among key microphysical properties. To further examine the microphysical features and physical processes, more cases need to be analyzed; eight fog events in 2007 are examined in this study.

The rest of the paper is organized. Section 2 briefly describes the observation site, the key instruments and the data. Section 3 presents the main results, including the general features of key microphysical properties and their mutual relationships under different conditions, and the discussion on the main and minor microphysical processes. Concluding remarks are presented in Section 4.

## **2. Observation site and data**

The sampling site is located at Pancheng (32°12'N, 118°42'E; 22 m above sea level) in the Nanjing area, Jiangsu Province, China; this area is unique from several perspectives. It is located to the north of the Yangtze River and adjacent to the Jiajiang River, which is the tributary of the Yangtze River. Furthermore, it is close to heavy pollution sources such as petrochemical factories, a steel plant, a thermal power station, a nitrogenous fertilizer plant, and highways. Further details can be found in Lu et al. (2010a). The data used in this study were collected from 15 November through 29 December 2007.

Similar to the observations at the same site in 2006 (Niu et al., 2010b), visibility was automatically measured and recorded every 15 s by a visibility meter (ZQZ-DN; the Radio Scientific Research Institute, Wuxi, Jiangsu, China); surface meteorological quantities (surface air temperature, relative humidity, wind speed, and wind direction) were observed with an automatic weather station (EnviroStation™, ICT International Pty Ltd, Armidale, New South Wales, Australia); the size distributions of fog droplets were measured with a droplet spectrometer (FM-100; Droplet Measurement Technologies, Colorado, USA) (Eugster et al., 2006; Gultepe et al., 2009). It measures fog droplets of 0.5–25  $\mu\text{m}$  in radius at a sampling rate of 1Hz, but the data from the bin 0.5-1.0  $\mu\text{m}$  are thought to be noisy, which are not included in the calculations of microphysical properties [ $N$ , mean radius ( $r_m$ ), standard deviation ( $\sigma$ ), LWC]. The dataset is averaged to 1 min for this work.

### 3. Results

#### 3.1 General microphysical characteristics

A total of eight typical dense fogs were observed during the campaign in 2007. Table 1 shows the duration time, the surface air temperature, and the microphysical properties in these cases. The durations of these cases are in the range of 4.3 - 25.3 h, and all the cases except the case 7 have severe fog periods which are defined in light of visibility  $< 50$  m (China Meteorological Association, 2007). According to the review of fog research by Gultepe et al. (2007), Petterssen (1956) suggested that fog can be divided into three subsections: Liquid fog (temperature  $> -10^{\circ}\text{C}$ ), mixed phase fog ( $-30^{\circ}\text{C} < \text{temperature} < -10^{\circ}\text{C}$ ), and ice fog (temperature  $< -30^{\circ}\text{C}$ ); it follows that the events observed in our experiments are all liquid fogs with average temperature above  $0^{\circ}\text{C}$ .

In every case,  $N$ , LWC,  $r_m$  and  $\sigma$  have large standard deviations due to both fog spatial inhomogeneous structure (García-García et al., 2002) and fog temporal evolution in different stages in every event. Peak radius ( $r_p$ ) is unique, always at  $1.4 \mu\text{m}$ ; this peak is not a real peak because it is at the first bin, but we still call it “peak” for convenience; similar spectral shape was also observed by García-García and Montanez (1991) and Gonser (2011); more discussion about the formation of the peak will be given later. Because of the peak at the first bin, the average values of  $r_m$  are smaller than the results observed in Sierra Madre Oriental, Mexico (García-García and Montañez, 1991) and in Pico del Este, Puerto Rico (Eugster et al., 2006). Although the average  $N$  is generally comparable with the results reported by Gultepe et al. (2009), the maximum  $N$  (around  $800 \text{ cm}^{-3}$ ) is much higher, caused by the high pollution level at this site (Lu et al., 2010a; Yang et al., 2011). Generally, the average LWC is comparable with the fogs in Pico del Este, Puerto Rico (Eugster et al., 2006) and Fichtelgebirge, Germany (Thalmann et al., 2002). Compared with the fog at the same site in 2006 (Niu et al., 2010b), the cases in this study have the same  $r_p$ , smaller  $N$ , LWC,  $r_m$ , and  $\sigma$ . It is noteworthy to point out that the observations in the above comparisons used the same droplet spectrometer (FM-100) except the observation in Sierra Madre Oriental, Mexico which used Forward Scattering Spectrometer Probe (FSSP) (García-García and Montañez, 1991); however, FSSP is similar to FM-100. Similar or same instruments assure the comparisons more reliable.

### 3.2 The dominant microphysical processes

As mentioned above, fog/cloud size distributions and hence the key microphysical properties ( $N$ , LWC,  $r_m$ ,  $\sigma$ ) are determined by different physical mechanisms; different relationships among these microphysical properties are expected in response to different physical mechanisms (Liu et al., 2008). Therefore, to examine the physical mechanisms, microphysical relationships among  $N$ , LWC,  $r_m$  and  $\sigma$  are analyzed. Table 2 shows that these relationships are all positive in the eight cases; Fig. 1 shows the case 6 as an example; the reason for choosing case 6 is that generally speaking, the values of microphysical properties (Table 1) and correlation coefficients (Table 2) in this case are in the middle of the eight cases, so this case is expected to well represent the eight cases. The positive relationship between  $r_m$  and  $N$  is opposite to some previous fog observations (e.g., Huang et al., 2000; Niu et al., 2010c; Li et al., 2011) or cloud observations (e.g., Wang et al., 2009). Collision-coalescence is not likely to be responsible for such a phenomenon, because if dominantly affected by collision-coalescence, droplet size (e.g.,  $r_m$ ) is expected to be negatively correlated with  $N$ . Turbulent entrainment-mixing processes are important factors affecting fog/cloud size distributions (e.g., Paluch and Baumgardner, 1989; Andrejczuk et al., 2009; Lu et al., 2011), but they are still not likely to dominate here, because the relationships of  $\sigma$  to  $N$ ,  $r_m$ , and LWC and the relationships of LWC to  $N$  and  $r_m$  are positive, while during entrainment-mixing processes,  $r_m$ ,  $N$ , LWC and  $\sigma$  are not likely to vary simultaneously (e.g., Liu et al., 2002; Wang et al., 2009). Therefore, the dominant processes seem to be droplet activation with subsequent condensational growth and/or droplet deactivation via some complete droplet evaporation. Similar conclusion is also drawn in the fog case in 2006 (Niu et al., 2010b). In addition, the fog in situ observation at Wuqing (39°24'N, 117°03'E) between two megacities, Beijing and Tianjing in China, also shows positive relationships between liquid water content to droplet number concentration and droplet size in three polluted fog cases (Quan et al., 2011).

To further discern the factors affecting microphysical relationships, the dataset is divided into two groups for every case based on visibility: mature stage ( $0 \text{ m} < \text{visibility} \leq 500 \text{ m}$ ) and formation/dissipation stage ( $500 \text{ m} < \text{visibility} < 1000 \text{ m}$ ). In the mature stage

in each case, the relationships among the key microphysical properties are all positive; whereas in the formation/dissipation stage, the relationships are complicated:  $r_m$  vs.  $N$  and  $\sigma$  vs.  $N$  are negatively correlated, and  $\sigma$  vs.  $r_m$  and LWC vs.  $N$  are positively correlated in each case; the relationships of  $\sigma$  vs. LWC and LWC vs.  $r_m$  are different from case to case, negatively, positively, or not correlated. As an example, Fig. 2 shows the microphysical relationships for these two visibility groups in the case 6. Compared with the mature stages and the whole fog dataset (Table 2, Fig. 1), the different behaviors of microphysical relationships in the formation/dissipation stages are likely related to the low and almost constant LWC. The LWC is a measure of available water vapor in air which can be condensed into liquid water under a certain environmental condition, such as water vapor mixing ratio, air temperature and air pressure. The competition for the limited LWC is expected to be remarkable because fog condensation nuclei are considered as sufficient due to the pollutant emission from the nearby industrial park (Lu et al., 2010a) and high water-soluble fraction of aerosol in this area (Wang et al., 2002, 2003). As a result, most droplets are small droplets and concentrated in the first bin (Fig. 3), decreasing the  $r_m$  and  $\sigma$  with an increase in the  $N$ . The complicated relationship of LWC to other properties is also probably related to the nearly constant LWC. Whereas in the mature stages, the LWC is positively correlated to the  $N$ ,  $\sigma$ , and  $r_m$  (Fig. 2), indicating that the available water vapor is sufficient and the competition for water vapor is expected to be weak. Therefore, the LWC is an important factor affecting the effect of the dominant processes (droplet activation with subsequent condensational growth and/or droplet deactivation via some complete droplet evaporation) on microphysical relationships. Zhang et al. (2011) also found that the value of LWC greatly affects the nucleation of aerosol, cloud number concentration and droplet size.

### **3.3 The combined effect of the dominant processes and collision-coalescence**

The dominance of droplet nucleation with subsequent condensational growth and/or droplet deactivation via some complete droplet evaporation cannot rule out the roles of other mechanisms. Fog explosive development is a frequent phenomenon (Pu et al., 2008; Lu et al., 2010b; Niu et al., 2011) with a sharp decrease in visibility to below 50 m during a

short time (e.g., 30 min); an example during a period in the case 6 is shown in Figs. 4 and 5. The LWC,  $N$ ,  $r_m$ ,  $\sigma$ , and maximum radius ( $r_{\max}$ ) remarkably increase during 0140 - 0150 LST (LST=UTC+8 h); correspondingly, the size distributions broaden quickly. It is noteworthy to mention that it takes only 4 minutes to formulate the droplets with  $r_{\max}$  around 15  $\mu\text{m}$  (0144 LST) from the droplets with  $r_{\max}$  around 7  $\mu\text{m}$  (0140 LST). Similar explosive developments were also observed in previous fog experiments (Wobrock et al., 1992). Furthermore, some  $r_{\max}$  values are even larger than 20  $\mu\text{m}$  (Fig. 4f) and Fig. 3 Fig. shows the average size distributions in the mature stage have  $r_{\max}$  in the range of 24-25  $\mu\text{m}$ . It is not likely that condensation is the only mechanism responsible for the formation of big droplets because condensational growth rate of droplet size is negatively correlated to droplet size itself (e.g., Rogers and Yau, 1989) and supersaturation in fog is often low (e.g., Hudson, 1980); collision-coalescence is likely to be important, although not dominating. It is often thought that gravitational collision-coalescence could not proceed until the radius of droplets exceeds 20  $\mu\text{m}$  (e.g., Jonas, 1996; Yum, 1998). The appearance of larger droplets (radius > 20  $\mu\text{m}$ ) shows the possibility of the occurrence of gravitational collision-coalescence. To further explore the effect of gravitational collision-coalescence intensity on the microphysical relationships, autoconversion threshold function ( $T$ ) proposed by Liu et al. (2005, 2006) is calculated for all the cases (see appendix for details). A larger value of  $T$  indicates a stronger collision-coalescence process, ranging from no action ( $T = 0$ ) to full action ( $T = 1$ ). Result shows that six out of eight cases have  $T$  smaller than 0.2, i.e., gravitational collision-coalescence is weak for most cases; but still, for the cases 2 and 6, the maximum values of  $T$  are 0.57 and 0.80, respectively, showing the importance of gravitational collision-coalescence in the two cases. In addition to gravitational collision-coalescence, Xue et al. (2008) and Ghosh et al. (2005) pointed out that turbulence could significantly enhance the collision rate for cloud droplets (> 10  $\mu\text{m}$  in radius). Therefore, except for the dominant mechanisms, the collision-coalescence is also an important mechanism in fog processes, especially the turbulent collision-coalescence.

To address the combined effects of the dominant processes and collision-coalescence in detail, the mature stages (500 m < visibility < 1000 m) are further divided into four groups based on visibility (0 m < visibility  $\leq$  50 m, 50 m < visibility  $\leq$  100 m, 100 m < visibility  $\leq$

200 m, and  $200 \text{ m} < \text{visibility} \leq 500 \text{ m}$ ). Generally, the microphysical relationships are kept positive for the four visibility groups in all the cases except the cases 2 and 8; as an example, Fig. 6 shows the relationships for the five visibility groups in the case 6; Figure 7 further shows that the size distributions broaden in the case 6 with a decrease in visibility, thus we assume collision-coalescence becomes more and more vigorous with decreasing visibility. During collision-coalescence, the formation of big droplets consumes small ones, tending to cause increases in  $r_m$ ,  $\sigma$  and a decrease in  $N$ . However, the relationships of  $r_m$  vs.  $N$  and  $\sigma$  vs.  $N$  are not negative; we argue that this is likely due to the reproduction of small droplets, which can compensate the loss of small droplets during collision-coalescence and results in synchronous increases in  $N$ ,  $r_m$  and  $\sigma$ . The reproduction can be caused by the growth of droplets with radius less than  $1 \mu\text{m}$ . As mentioned above, the droplets with radius in the range of  $0.5\text{-}1 \mu\text{m}$  can be measured by the spectrometer, but not included in the calculations of microphysical properties because the data of this bin are thought to be noisy. However, they can still give some hints; the number concentration of this bin is always larger than the value at the current peak at  $1.4 \mu\text{m}$  in radius, so it is important that the reproduction of small droplets is through the growth of droplets in the range of  $0.5\text{-}1 \mu\text{m}$  in radius. Furthermore, the high concentration of droplets with radius in the range of  $0.5\text{-}1 \mu\text{m}$  always exists, which could be caused by the nucleation of sufficient fog condensation nuclei and subsequent condensation. The positive relationships of LWC to  $\sigma$ ,  $N$ , and  $r_m$  (Fig. 6d, e, f) indicate that there is sufficient LWC which could enhance the nucleation of aerosol (Zhang et al., 2011). The reproduction of small droplets confirms the dominant processes identified above and causes the stable peak radius at  $1.4 \mu\text{m}$ . Therefore, the sufficient fog condensation nuclei in the polluted area, along with the higher LWC, is important for the positive relationships of  $r_m$  vs.  $N$  and  $\sigma$  vs.  $N$ . Similar phenomena were also presented by Hudson and Svensson (1995); they analyzed the cloud microphysical properties off the southern California coast and found that in three cases which had larger cloud condensation nuclei due to the effect of ship exhaust plumes, the  $r_m$  and  $N$  showed positive relationships, whereas for other cases, the relationship was negative. Furthermore, Wang et al. (2009) examined the marine clouds observed off the coast of Monterey and Point Reyes, northern California with data reflecting ship exhaust plumes deleted, and

found negative relationship between  $r_m$  and  $N$ ; the average size distributions along different flight horizontal levels showed small number concentration of small droplets, indicative of not sufficient reproduction of small droplets by nucleation after cloud formation.

However, negative relationships of  $r_m$  vs.  $N$  and  $\sigma$  vs.  $N$  are found for  $0 \text{ m} < \text{visibility} \leq 50 \text{ m}$  in the case 2 (not shown) and for  $0 \text{ m} < \text{visibility} \leq 100 \text{ m}$  in the case 8 (Fig. 8). The reasons for the negative relationships here are different from the negative relationships for  $500 \text{ m} < \text{visibility} < 1000 \text{ m}$  shown above, which are due to the competition for nearly constant LWC and sufficient fog condensation nuclei; whereas here the LWC is not close to a constant as indicated by the positive relationships of  $\sigma$  vs. LWC, LWC vs.  $N$ , and LWC vs.  $r_m$  (Fig. 8d, e, f). Furthermore, with a decrease in visibility, the relationships of  $r_m$  vs.  $N$  and  $\sigma$  vs.  $N$  change from positive relationship ( $200 \text{ m} < \text{visibility} \leq 500 \text{ m}$ ) to irrelevance ( $100 \text{ m} < \text{visibility} \leq 200 \text{ m}$ ), and then to negative relationship ( $50 \text{ m} < \text{visibility} \leq 100 \text{ m}$  and  $0 \text{ m} < \text{visibility} \leq 50 \text{ m}$ ). Similar conclusion can be drawn in the case 2.

We argue that whether  $r_m$  vs.  $N$  and  $\sigma$  vs.  $N$  are positively, negatively, or not correlated in all the eight cases depends on the competition between the loss of small droplets due to collision-coalescence and the compensation of small droplets due to nucleation and condensation; generally, compensation is larger than the loss because six cases have positive relationships for lower visibility compared with only two cases which have negative relationships. The variation of coefficient in the latter two cases (cases 2 and 8) is consistent with the assumption that collision-coalescence becomes more and more vigorous with the decreasing visibility, which causes a larger loss of small droplets than compensation.

In the above discussion, turbulent and gravitational collision-coalescence processes are assumed to occur more vigorously for lower visibility. Based on  $T$ , the effect of gravitational collision-coalescence can be further studied. The data in the cases 2 and 6, which have  $T$  larger than 0.2, are divided based on  $T$  ranges ( $0 \leq T \leq 0.2$ ,  $0.2 < T < 0.6$  and  $0.6 \leq T \leq 1.0$ ). Figure 9 shows the case 6 as an example. The negative relationships of  $r_m$  vs.  $N$  and  $\sigma$  vs.  $N$  for higher  $T$  show that the loss of small droplets due to gravitational collision-coalescence is expected to be higher than the compensation. Similar phenomenon is found in the case 2 although it has only two  $T$  ranges ( $0 \leq T \leq 0.2$ ,  $0.2 < T < 0.6$ ).

Furthermore, it is interesting to find that  $r_m$  vs.  $N$  and  $\sigma$  vs.  $N$  are negative for  $0.2 < T \leq 1.0$  (Fig. 9a, b) but positive for  $0 \text{ m} < \text{visibility} \leq 50 \text{ m}$  (Fig. 6a, b) in the case 6. Comparison of the two figures indicates that the data points with  $0 \text{ m} < \text{visibility} \leq 50 \text{ m}$  are much more than those with  $0.2 < T \leq 1.0$ . Therefore only a few size distributions are affected by gravitational collision-coalescence; most droplet spectral broadening is likely related to turbulent collision-coalescence. The reproduction of small droplets can compensate the loss of small droplets due to turbulence collision-coalescence but not gravitational collision-coalescence. In addition, all the microphysical relationships in the higher  $T$  groups generally have weak positive relationships, or even irrelevances, negative relationships. Similar conclusion was also drawn in the fog in 2006 that gravitational collision-coalescence tends to destroy some of the positive relationships induced by the dominant processes in fog process (Niu et al., 2010b).

#### 4. Concluding remarks

Warm fog microphysics is examined using the in situ observations conducted at Pancheng, Nanjing, China in 2007. Through the analysis of different microphysical relationships in the eight fog cases, the microphysical processes and key factors affecting fog microphysics are explored.

It is demonstrated that the key microphysical properties [droplet number concentration ( $N$ ), mean radius ( $r_m$ ), spectral standard deviation ( $\sigma$ ), liquid water content (LWC)] in the eight cases all exhibit positive relationships with one another, indicating that the dominant microphysical process is likely to be droplet activation with subsequent condensational growth and/or droplet deactivation via some complete droplet evaporation. The LWC is a key factor affecting the effect of the dominant processes on microphysical relationships. In the formation/dissipation stages ( $500 \text{ m} < \text{visibility} < 1000 \text{ m}$ ),  $\sigma$  vs.  $N$  and  $r_m$  vs.  $N$  are negatively correlated due to the competition of sufficient fog condensation nuclei for nearly constant LWC; in the mature stages ( $0 \text{ m} < \text{visibility} \leq 500 \text{ m}$ ), the LWC is not close to a constant, but positively correlated to  $N$ ,  $\sigma$ , and  $r_m$ ; as a result, the competition for LWC is not remarkable and  $\sigma$  vs.  $N$  and  $r_m$  vs.  $N$  are positively correlated.

Besides the dominant mechanism, the fog explosive development along with abrupt broadening of fog size distributions indicates that turbulent and gravitational collision-coalescence processes are also important, although not dominating. The mature stages ( $0 \text{ m} < \text{visibility} \leq 500 \text{ m}$ ) are further divided into four groups ( $0 \text{ m} < \text{visibility} \leq 50 \text{ m}$ ,  $50 \text{ m} < \text{visibility} \leq 100 \text{ m}$ ,  $100 \text{ m} < \text{visibility} \leq 200 \text{ m}$ , and  $200 \text{ m} < \text{visibility} \leq 500 \text{ m}$ ). Positive relationships among LWC,  $N$ ,  $r_m$ , and  $\sigma$  hold in the four visibility ranges for six cases; in the other two cases (cases 2 and 8), LWC vs.  $N$ , LWC vs.  $r_m$ ,  $\sigma$  vs. LWC, and  $\sigma$  vs.  $r_m$  are positive, but the relationships of  $r_m$  vs.  $N$  and  $\sigma$  vs.  $N$  are found from positive relationship, to irrelevance, and to negative relationship with the decreasing visibility, indicating more and more vigorous collision-coalescence. We argue that the complicated relationships of  $r_m$  vs.  $N$  and  $\sigma$  vs.  $N$  are closely related to the competition between the loss of small droplets due to collision-coalescence and the compensation of small droplets due to nucleation and condensation. Generally, the compensation is larger than the loss because of the large concentration of fog condensation nuclei in this polluted area.

To further explore the effect of gravitational collision-coalescence, autoconversion threshold function ( $T$ ) is calculated. Among the eight cases, the cases 2 and 6 have  $T$  larger than 0.2 and the dataset is divided based on  $T$  ranges ( $0 \leq T \leq 0.2$ ,  $0.2 < T < 0.6$  and  $0.6 \leq T \leq 1.0$ ), negative relationships of  $r_m$  vs.  $N$  and  $\sigma$  vs.  $N$  are found for larger  $T$ . Furthermore, with the increasing  $T$ , correlation coefficients of  $\sigma$  vs.  $r_m$ ,  $\sigma$  vs. LWC, LWC vs.  $N$  and LWC vs.  $r_m$  become less positive or even negative. The gravitational collision-coalescence tends to weaken the positive relationships among key microphysical properties caused by the dominant processes.

It is noteworthy to point out that this study focuses on the fog microphysics; the analysis on macrophysical processes is not sufficient. But macro conditions for the fog formation, duration, and dissipation are important to understand the microphysical processes. For example, as mentioned above, the LWC is greatly affected by some environmental conditions (such as water vapor mixing ratio, air temperature, and air pressure), which are further related to radiation, turbulence, and etc (e.g., Zhou and Ferrier, 2008). Therefore, detailed analysis on the macro mechanisms responsible for fog formation is necessary in the future study.

## Appendix. Autoconversion threshold function

According to Liu et al. (2005, 2006), all the autoconversion parameterizations that have been developed so far can be generically written as:

$$P=P_0T, \quad (\text{A.1})$$

where  $P$  is the autoconversion rate,  $P_0$  is the rate function describing the conversion rate after the onset of the autoconversion process, and  $T$  is the threshold function describing the threshold behavior of the autoconversion process. The size truncation function employed to quantify the effect of truncating the cloud droplet size distribution on the autoconversion rate can be used as a threshold function to represent the threshold behavior associated with the autoconversion process, providing a physical basis for the threshold function. The expression of  $T$  can be generally described by:

$$T = \frac{P}{P_0} = \frac{\left[ \frac{\int_{r_c}^{\infty} r^6 n(r) dr}{\int_0^{\infty} r^6 n(r) dr} \right]}{\left[ \frac{\int_{r_c}^{\infty} r^3 n(r) dr}{\int_0^{\infty} r^3 n(r) dr} \right]}, \quad (\text{A.2})$$

where  $r$  is the droplet radius,  $n(r)$  is the cloud/fog droplet size distribution, and  $r_c$  is the critical radius for autoconversion. Liu et al. (2004) derived an analytical expression for predicting  $r_c$  in the autoconversion parameterization:

$$r_c \approx 4.09 \times 10^{-4} \beta_{\text{con}}^{1/6} \frac{N^{1/6}}{LWC^{1/3}}, \quad (\text{A.3})$$

where  $\beta_{\text{con}} = 1.15 \times 10^{23}$  is an empirical coefficient.

## **Acknowledgments**

Lu and Liu are supported by the DOE Earth System Modeling (ESM) program via the FASTER project ([www.bnl.gov/esm](http://www.bnl.gov/esm)) and Atmospheric System Research (ASR) program. Niu and Zhao are supported by the National Natural Science Foundation of China (Grant Nos. 40537034 and 40775012) and the Qing-Lan Project for Cloud-Fog-Precipitation-Aerosol Study in Jiangsu Province, China.

## **References**

- Andrejczuk, M., Grabowski, W.W., Malinowski, S.P., Smolarkiewicz, P.K., 2009. Numerical simulation of cloud-clear air interfacial mixing: Homogeneous versus inhomogeneous mixing. *Journal of the Atmospheric Sciences* 66, 2493-2500.
- Baumgardner, D., Baker, B., Weaver, K., 1993. A technique for the measurement of cloud structure on centimeter scales. *Journal of Atmospheric and Oceanic Technology* 10, 557-565.
- Bergot, T., Carrer, D., Noilhan, J., Bougeault, P., 2005. Improved site-specific numerical prediction of fog and low clouds: A feasibility study. *Weather and Forecasting* 20, 627-646.
- Bergot, T., Guedalia, D., 1994. Numerical forecasting of radiation fog. Part I: numerical model and sensitivity tests. *Monthly Weather Review* 122, 1218-1230.
- Bott, A., Sievers, U., Zdunkowski, W., 1990. A radiation fog model with a detailed treatment of the interaction between radiative transfer and fog microphysics. *Journal of the Atmospheric Sciences* 47, 2153-2166.
- Burnet, F., Brenguier, J.L., 2007. Observational study of the entrainment-mixing process in warm convective clouds. *Journal of the Atmospheric Sciences* 64, 1995-2011.
- China Meteorological Association, 2007. Specifications for surface meteorological observation. Part4: Observation of weather phenomenon (QX/T 48-2007), Beijing. (in Chinese)
- Croft, P.J., Pfoft, R.L., Medlin, J.M., Johnson, G.A., 1997. Fog forecasting for the southern region: A conceptual model approach. *Weather and Forecasting* 12, 545-556.

- Duynkerke, P.G., 1991. Observation of a quasi-periodic oscillation due to gravity waves in a shallow radiation fog. *Quarterly Journal of the Royal Meteorological Society* 117, 1207-1224.
- Eldridge, R.G., 1961. A few fog drop-size distributions. *Journal of Meteorology* 18, 671-676.
- Eldridge, R.G., 1971. The relationship between visibility and liquid water content in fog. *Journal of the Atmospheric Sciences* 28, 1183-1186.
- Eugster, W., Burkard, R., Holwerda, F., Scatena, F.N., Bruijnzeel, L.A., 2006. Characteristics of fog and fogwater fluxes in a Puerto Rican elfin cloud forest. *Agricultural and Forest Meteorology* 139, 288-306.
- Fu, G., Guo, J., Pendergrass, A., Li, P., 2008. An analysis and modeling study of a sea fog event over the Yellow and Bohai Seas. *Journal of Ocean University of China (English Edition)* 7, 27-34.
- Fu, G., Guo, J., Xie, S.-P., Duan, Y., Zhang, M., 2006. Analysis and high-resolution modeling of a dense sea fog event over the Yellow Sea. *Atmospheric Research* 81, 293-303.
- Fuzzi, S., Facchini, M.C., Orsi, G., Lind, J.A., Wobrock, W., Kessel, M., Maser, R., Jaeschke, W., Enderle, K.H., Arends, B.G., Berner, A., Solly, I., Krusisz, C., Reischl, G., Pahl, S., Kaminski, U., Winkler, P., Ogren, J.A., Noone, K.J., Hallberg, A., Fierlinger-Oberlinninger, H., Puxbaum, H., Marzorati, A., Hansson, H.C., Wiedensohler, A., Svenningsson, I.B., Martinsson, B.G., Schell, D., Georgii, H.W., 1992. The Po Valley fog experiment 1989. *Tellus B* 44, 448-468.
- Gao, S., Lin, H., Shen, B., Fu, G., 2007. A heavy sea fog event over the Yellow Sea in March 2005: Analysis and numerical modeling. *Advances in Atmospheric Sciences* 24, 65-81.
- García-García, F., Montañez, R.A., 1991. Warm fog in eastern Mexico: A case study. *Atmósfera* 4, 53-64.
- García-García, F., Virafuentes, U., Montero-Martínez, G., 2002. Fine-scale measurements of fog-droplet concentrations: A preliminary assessment. *Atmospheric Research* 64, 179-189.

- Gerber, H., 1991. Supersaturation and droplet spectral evolution in fog. *Journal of the Atmospheric Sciences* 48, 2569-2588.
- Ghosh, S., Dávila, J., Hunt, J.C.R., Srdic, A., Fernando, H.J.S., Jonas, P.R., 2005. How turbulence enhances coalescence of settling particles with applications to rain in clouds. *Proceedings of the Royal Society (A)* 461, 3059-3088.
- Gonser, S., Klemm, O., Griessbaum, F., Chang, S.-C., Chu, H.-S., Hsia, Y.-J., 2011. The relation between humidity and liquid water content in fog: An experimental approach. *Pure and Applied Geophysics* (In Press).
- Gultepe, I., Milbrandt, J.A., 2007. Microphysical Observations and Mesoscale Model Simulation of a Warm Fog Case during FRAM Project. *Pure and Applied Geophysics* 164, 1161-1178.
- Gultepe, I., Pearson, G., Milbrandt, J.A., Hansen, B., Platnick, S., Taylor, P., Gordon, M., Oakley, J.P., Cober, S.G., 2009. The fog remote sensing and modeling field project. *Bulletin of the American Meteorological Society* 90, 341-359.
- Gultepe, I., Tardif, R., Michaelides, S.C., Cermak, J., Bott, A., Bendix, J., Müller, M.D., Pagowski, M., Hansen, B., Ellrod, G., Jacobs, W., Toth, G., Cober, S.G., 2007. Fog research: A review of past achievements and future perspectives. *Pure and Applied Geophysics* 164, 1121-1159.
- Haefelin, M., Bergot, T., Elias, T., Tardif, R., Carrer, D., Chazette, P., Colomb, M., Drobinski, P., Dupont, E., Dupont, J.-C., Gomes, L., Musson-Genon, L., Pietras, C., Plana-Fattori, A., Protat, A., Rangognio, J., Raut, J.-C., Rémy, S., Richard, D., Sciare, J., Zhang, X., 2010. PARISFOG: Shedding new light on fog physical processes. *Bulletin of the American Meteorological Society* 91, 767-783.
- Haman, K.E., Malinowski, S.P., Kurowski, M.J., Gerber, H., Brenguier, J.-L., 2007. Small scale mixing processes at the top of a marine stratocumulus - a case study. *Quarterly Journal of the Royal Meteorological Society* 133, 213-226.
- He, Y., Zhu, B., Ma, L., 2003. The physical process of Chongqing fog's genesis and dissipation in winter. *Journal of Nanjing Institute of Meteorology* 26, 821-828.

- Hong, Z., Huang, M., 1965. The second maximum and other related characteristics of the Southern Mountain cloud spectra, In: Zhao, J. (Eds.), *The Study on Microphysics of Cloud/Fog Precipitation in China*, Science Press, Beijing, China, pp. 18-29. (in Chinese)
- Huang, Y., Huang, Y., Li, Z., Chen, B., Huang, J., Gu, J., 2000. The microphysical structure and evolution of winter fog in Xishuangbanna. *Acta Meteorologica Sinica* 58, 715-725. (in Chinese)
- Hudson, J.G., 1980. Relationship between fog condensation nuclei and fog microstructure. *Journal of the Atmospheric Sciences* 37, 1854-1867.
- Hudson, J.G., Svensson, G., 1995. Cloud microphysical relationships in California marine stratus. *Journal of Applied Meteorology* 34, 2655-2666.
- Justo, J.E., Lala, G.G., 1980. Radiation fog formation and dissipation: a case study. *Journal de Recherches Atmospheriques* 14, 391-397.
- Jonas, P.R., 1996. Turbulence and cloud microphysics. *Atmospheric Research* 40, 283-306.
- Kim, C.K., 2011. An observational and numerical study of sea fog formation off the west coast of the Korean Peninsula, Ph. D. thesis, Yonsei University, Seoul, Korea.
- Klemm, O., Wrzesinsky, T., 2007. Fog deposition fluxes of water and ions to a mountainous site in Central Europe. *Tellus: Series B* 59, 705-714.
- Kong, F., 2002. An experimental simulation of a coastal fog-stratus case using COAMPS(tm) model. *Atmospheric Research* 64, 205-215.
- Kunkel, B.A., 1984. Parameterization of droplet terminal velocity and extinction coefficient in fog models. *Journal of Climate and Applied Meteorology* 23, 34-41.
- Li, P., Li, X., Yang, C., Wang, X., Chen, J., Collett Jr, J.L., 2011. Fog water chemistry in Shanghai. *Atmospheric Environment* 45, 4034-4041.
- Li, Z., 2001. Study of fog in China over the past 40 years. *Acta Meteorologica Sinica* 59, 616-624. (in Chinese)
- Liu, Y., Daum, P.H., Chai, S.K., Liu, F., 2002. Cloud parameterizations, cloud physics, and their connections: An overview. *Recent Res. Devel. Geophysics* 4, 119-142.

- Liu, Y., Daum, P.H., McGraw, R., 2004. An analytical expression for predicting the critical radius in the autoconversion parameterization. *Geophysical Research Letter* 31, L06121.
- Liu, Y., Daum, P.H., McGraw, R., 2005. Size truncation effect, threshold behavior, and a new type of autoconversion parameterization. *Geophysical Research Letter* 32, L11811.
- Liu, Y., Daum, P.H., McGraw, R., Miller, M., 2006. Generalized threshold function accounting for effect of relative dispersion on threshold behavior of autoconversion process. *Geophysical Research Letter* 33, L11804.
- Liu, Y., Daum, P.H., Yum, S.S., Wang, J., 2008. Use of microphysical relationships to discern growth/decay mechanisms of cloud droplets with focus on Z-LWC relationships. 15th International Conference on Clouds and Precipitation, Cancun, Mexico, the International Commission on Clouds and Precipitation (ICCP).
- Lu, C., Liu, Y., Niu, S., 2011. Examination of turbulent entrainment-mixing mechanisms using a combined approach. *Journal of Geophysical Research* (In press).
- Lu, C., Niu, S., 2008. Study on microphysical characteristics of winter fog in Nanjing area, China. 2008 International Workshop on Education Technology and Training & 2008 International Workshop on Geoscience and Remote Sensing, Shanghai, China, IEEE Computer Society, USA 273-276.
- Lu, C., Niu, S., Tang, L., Lü, J., Zhao, L., Zhu, B., 2010a. Chemical composition of fog water in Nanjing area of China and its related fog microphysics. *Atmospheric Research* 97, 47-69.
- Lu, C., Niu, S., Yang, J., Liu, X., Zhao, L., 2010b. Jump features and causes of macro and microphysical structures of a winter fog in Nanjing. *Chinese Journal of Atmospheric Sciences* 34, 681-690. (in Chinese)
- Meyer, M.B., Jiusto, J.E., Lala, G.G., 1980. Measurements of visual range and radiation-fog (haze) microphysics. *Journal of the Atmospheric Sciences* 37, 622-629.
- Meyer, M.B., Lala, G.G., Jiusto, J.E., 1986. Fog-82: A Cooperative Field Study of Radiation Fog. *Bulletin of the American Meteorological Society* 67, 825-832.

- Niu, F., Li, Z., Li, C., Lee, K.-H., Wang, M., 2010a. Increase of wintertime fog in China: Potential impacts of weakening of the Eastern Asian monsoon circulation and increasing aerosol loading. *Journal of Geophysical Research* 115, D00K20.
- Niu, S., Liu, D., Zhao, L., Lu, C., Lü, J., Yang, J., 2011. Summary of a 4-year fog field study in northern Nanjing, part 2: Fog microphysics. *Pure and Applied Geophysics* (In Press).
- Niu, S., Lu, C., Liu, Y., Zhao, L., Lü, J., Yang, J., 2010b. Analysis of the microphysical structure of heavy fog using a droplet spectrometer: A case study. *Advances in Atmospheric Sciences* 27, 1259-1275.
- Niu, S., Lu, C., Yu, H., Zhao, L., Lü, J., 2010c. Fog research in China: An overview. *Advances in Atmospheric Sciences* 27, 639-661.
- Paluch, I.R., Baumgardner, D.G., 1989. Entrainment and fine-scale mixing in a continental convective cloud. *Journal of the Atmospheric Sciences* 46, 261-278.
- Petterssen, S., 1956. *Weather analysis and forecasting*, McGraw-Hill Publ. Inc., New York, USA.
- Pilié, R.J., Mack, E.J., Kocmond, W.C., Eadie, W.J., Rogers, C.W., 1975. The life cycle of valley fog. Part II: Fog microphysics. *Journal of Applied Meteorology* 14, 364-374.
- Pinnick, R.G., Hoihjelle, D.L., Fernandez, G., Stenmark, E.B., Lindberg, J.D., Hoidale, G.B., Jennings, S.G., 1978. Vertical structure in atmospheric fog and haze and its effects on visible and infrared extinction. *Journal of the Atmospheric Sciences* 35, 2020-2032.
- Porson, A., Price, J., Lock, A., Clark, P., 2011. Radiation fog. Part II: Large-eddy simulations in very stable conditions. *Boundary-Layer Meteorology*, 1-32.
- Price, J., 2011. Radiation fog. Part I: Observations of stability and drop size distributions. *Boundary-Layer Meteorology*, 1-25.
- Pu, M., Zhang, G., Yan, W., Li, Z., 2008. Features of a rare advection-radiation fog event. *Science in China Series D: Earth Sciences* 51, 1044-1052.
- Quan, J., Zhang, Q., He, H., Liu, J., Huang, M., Jin, H., 2011. Analysis of the formation of fog and haze in North China Plain (NCP). *Atmospheric Chemistry and Physics* 11, 8205-8214.

- Rémy, S., Bergot, T., 2010. Ensemble Kalman Filter data assimilation in a 1D numerical model used for fog forecasting. *Monthly Weather Review* 138, 1792-1810.
- Roach, W.T., 1976. On some quasi-periodic oscillations observed during a field investigation of radiation fog. *Quarterly Journal of the Royal Meteorological Society* 102, 355-359.
- Roach, W.T., Brown, R., Caughey, S.J., Garland, J.A., Readings, C.J., 1976. The physics of radiation fog: I – a field study. *Quarterly Journal of the Royal Meteorological Society* 102, 313-333.
- Rogers, R.R., Yau, M.K., 1989. *A short course in cloud physics*, Butterworth Heinemann, Burlington, MA, USA.
- Shi, C., Wang, L., Zhang, H., Zhang, S., Deng, X., Li, Y., Qiu, M., 2011. Fog simulations based on multi-model system: A feasibility study. *Pure and Applied Geophysics* (In Press).
- Shi, C., Yang, J., Qiu, M., Zhang, H., Zhang, S., Li, Z., 2010. Analysis of an extremely dense regional fog event in Eastern China using a mesoscale model. *Atmospheric Research* 95, 428-440.
- Stoelinga, M.T., Warner, T.T., 1999. Nonhydrostatic, mesobeta-scale model simulations of cloud ceiling and visibility for an east coast winter precipitation event. *Journal of Applied Meteorology* 38, 385-404.
- Stolaki, S., Pytharoulis, I., Karacostas, T., 2011. A study of fog characteristics using a coupled WRF–COBEL model over Thessaloniki airport, Greece. *Pure and Applied Geophysics* (In Press).
- Thalmann, E., Burkard, R., Wrzesinsky, T., Eugster, W., Klemm, O., 2002. Ion fluxes from fog and rain to an agricultural and a forest ecosystem in Europe. *Atmospheric Research* 64, 147-158.
- Thoma, C., Schneider, W., Masbou, M., Bott, A., 2011. Integration of local observations into the one dimensional fog model PAFOG. *Pure and Applied Geophysics* (In Press).

- Tomasi, C., Tampieri, F., 1976. Features of the proportionality coefficient in the relationship between visibility and liquid water content in haze and fog. *Atmosphere* 14, 61-76.
- Wang, G., Huang, L., Gao, S., Gao, S., Wang, L., 2002. Characterization of water-soluble species of PM10 and PM2.5 aerosols in urban area in Nanjing, China. *Atmospheric Environment* 36, 1299-1307.
- Wang, G., Wang, H., Yu, Y., Gao, S., Feng, J., Gao, S., Wang, L., 2003. Chemical characterization of water-soluble components of PM10 and PM2.5 atmospheric aerosols in five locations of Nanjing, China. *Atmospheric Environment* 37, 2893-2902.
- Wang, J., Daum, P.H., Yum, S.S., Liu, Y., Senum, G.I., Lu, M.-L., Seinfeld, J.H., Jonsson, H., 2009. Observations of marine stratocumulus microphysics and implications for processes controlling droplet spectra: Results from the Marine Stratus/Stratocumulus Experiment. *Journal of Geophysical Research* 114, D18210.
- Welch, R.M., Ravichandran, M.G., Cox, S.K., 1986. Prediction of quasi-periodic oscillations in radiation fogs. Part I: Comparison of simple similarity approaches. *Journal of the Atmospheric Sciences* 43, 633-651.
- Wendisch, M., Mertes, S., Heintzenberg, J., Wiedensohler, A., Schell, D., Wobrock, W., Frank, G., Martinsson, B.G., Fuzzi, S., Orsi, G., Kos, G., Berner, A., 1998. Drop size distribution and LWC in Po Valley fog. *Contributions to Atmospheric Physics* 71, 87-100.
- Wobrock, W., Schell, D., Maser, R., Kessel, M., Jaeschke, W., Fuzzi, S., Facchini, M.C., Orsi, G., Marzorati, A., Winkler, P., Arends, B.G., Bendix, J., 1992. Meteorological characteristics of the Po Valley fog. *Tellus B* 44, 469-488.
- Xue, Y., Wang, L.-P., Grabowski, W.W., 2008. Growth of cloud droplets by turbulent collision-coalescence. *Journal of the Atmospheric Sciences* 65, 331-356.
- Yang, D., Ritchie, H., Desjardins, S., Pearson, G., MacAfee, A., Gultepe, I., 2010. High-resolution GEM-LAM application in marine fog prediction: Evaluation and diagnosis. *Weather and Forecasting* 25, 727-748.

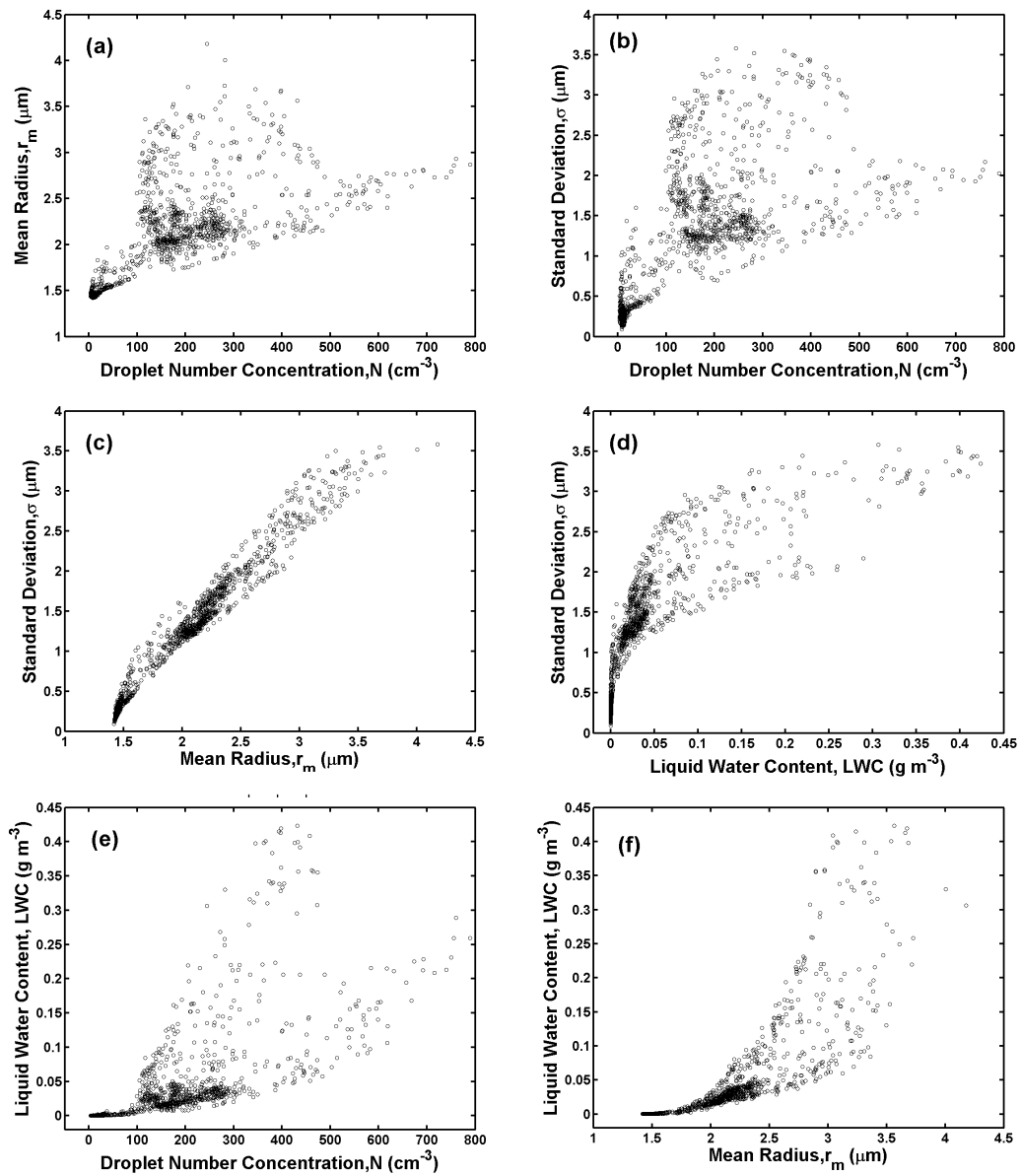
- Yang, J., Xie, Y.-J., Shi, C.-E., Liu, D.-Y., Niu, S.-J., Li, Z.-H., 2011. Ion composition of fog water and its relation to air pollutants during winter fog events in Nanjing, China. *Pure and Applied Geophysics* (In Press).
- Yum, S., 1998. Cloud droplet spectral broadening in warm clouds: An observational and model study, Ph. D. thesis, University of Nevada, Reno, Nevada, USA.
- Zhang, Q., Quan, J., Tie, X., Huang, M., Ma, X., 2011. Impact of aerosol particles on cloud formation: Aircraft measurements in China. *Atmospheric Environment* 45, 665-672.
- Zhou, B., Du, J., 2010. Fog prediction from a multimodel mesoscale ensemble prediction system. *Weather and Forecasting* 25, 303–322.
- Zhou, B., Du, J., Gultepe, I., Dimego, G., 2011. Forecast of low visibility and fog from NCEP: Current status and efforts. *Pure and Applied Geophysics* (In Press).
- Zhou, B., Ferrier, B.S., 2008. Asymptotic analysis of equilibrium in radiation fog. *Journal of Applied Meteorology & Climatology* 47, 1704-1722.

Table 1. The duration time, the surface air temperature, and the key microphysical properties in the eight fog cases. The figures in the parenthesis are the values of standard deviations of the corresponding properties; LST=UTC+8 h.

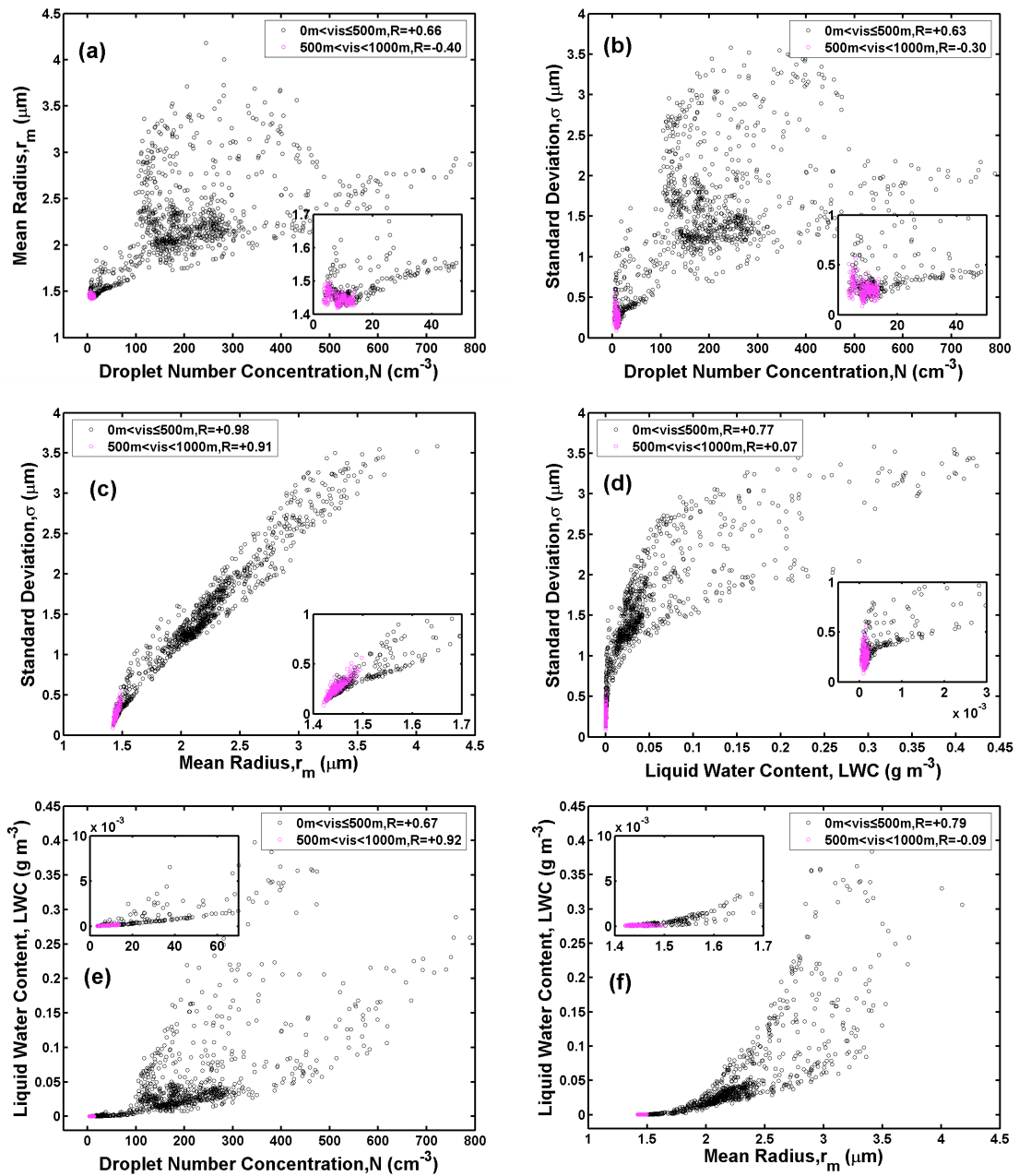
Case	Formation Time (LST)	Dissipation Time (LST)	Duration (h)	Duration of visibility < 50 m (h)	Temperature (°C)	Concentration $N(\text{cm}^{-3})$	Liquid water content LWC ( $\text{g m}^{-3}$ )	Mean radius $r_m$ ( $\mu\text{m}$ )	Spectral standard deviation $\sigma$ ( $\mu\text{m}$ )	Peak radius $r_p$ ( $\mu\text{m}$ )
1	12/10/2007 22:31	12/11/2007 12:30	14.0	2.0	3.8 (1.4)	64.2 (139.9)	0.022 (0.061)	1.8 (0.5)	0.9 (0.6)	1.4 (0)
2	12/13/2007 21:55	12/14/2007 11:20	13.5	4.3	0.6 (1.2)	172.6 (248.0)	0.074 (0.127)	2.0 (0.8)	1.0 (1.0)	1.4 (0)
3	12/14/2007 20:48	12/15/2007 12:02	15.2	0.8	2.2 (1.7)	21.6 (71.3)	0.001 (0.004)	1.6 (0.1)	0.7 (0.2)	1.4 (0)
4	12/18/2007 02:28	12/18/2007 11:11	8.7	1.8	4.0 (0.8)	81.7 (127.5)	0.021 (0.046)	1.7 (0.4)	0.8 (0.7)	1.4 (0)
5	12/18/2007 16:07	12/19/2007 12:28	20.4	6.5	3.8 (2.1)	128.9 (185.4)	0.041 (0.084)	1.9 (0.6)	1.0 (0.8)	1.4 (0)
6	12/19/2007 16:37	12/20/2007 16:11	23.6	13.0	4.6 (1.3)	138.7 (145.5)	0.037 (0.068)	2.0 (0.5)	1.1 (0.9)	1.4 (0)
7	12/20/2007 17:48	12/21/2007 19:06	25.3	0.0	7.7 (0.7)	39.5 (60.8)	0.003 (0.009)	1.6 (0.1)	0.6 (0.2)	1.4 (0)
8	12/23/2007 01:16	12/23/2007 05:30	4.3	1.3	5.6 (0.5)	140.5 (127.1)	0.040 (0.048)	2.3 (0.6)	1.6 (0.8)	1.4 (0)

Table 2. The correlation coefficients of the relationships among the key fog microphysical properties.

Case	$r_m$ vs. $N$	$\sigma$ vs. $N$	$\sigma$ vs. $r_m$	$\sigma$ vs. LWC	LWC vs. $N$	LWC vs. $r_m$
1	0.90	0.82	0.97	0.85	0.93	0.93
2	0.89	0.89	0.99	0.93	0.88	0.95
3	0.77	0.19	0.68	0.23	0.96	0.77
4	0.91	0.86	0.97	0.91	0.87	0.95
5	0.88	0.81	0.98	0.82	0.83	0.88
6	0.73	0.70	0.99	0.78	0.70	0.79
7	0.88	0.65	0.89	0.71	0.86	0.85
8	0.40	0.33	0.97	0.72	0.64	0.75



**Fig. 1** Relationships (a) between the mean radius ( $r_m$ ) and the droplet number concentration ( $N$ ), (b) between the standard deviation ( $\sigma$ ) and  $N$ , (c) between  $\sigma$  and  $r_m$ , (d) between the  $\sigma$  and the LWC, (e) between the LWC and the  $N$ , (f) between the LWC and the  $r_m$  in the case 6.



**Fig. 2** Relationships (a) between the mean radius ( $r_m$ ) and the droplet number concentration ( $N$ ), (b) between the standard deviation ( $\sigma$ ) and  $N$ , (c) between  $\sigma$  and  $r_m$ , (d) between the  $\sigma$  and the LWC, (e) between the LWC and the  $N$ , (f) between the LWC and the  $r_m$  for two visibility ( $vis$ ) ranges in the case 6. The enlarged figures are added.

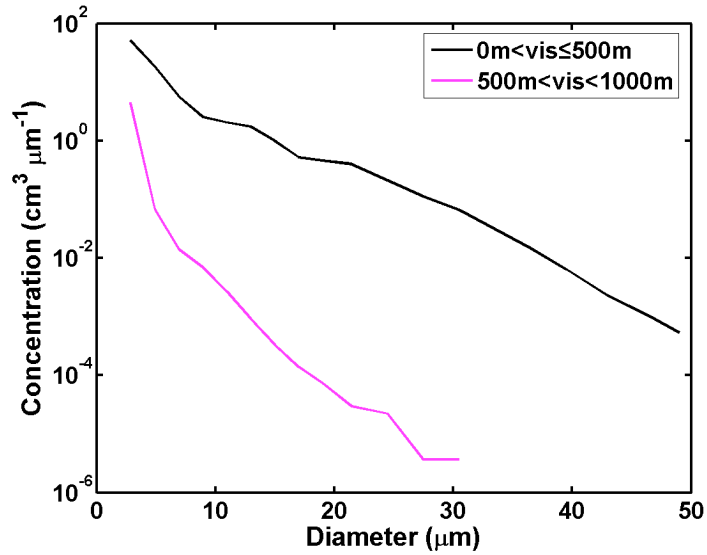


**Fig. 3** Average size distributions for two visibility ranges in the case 6.

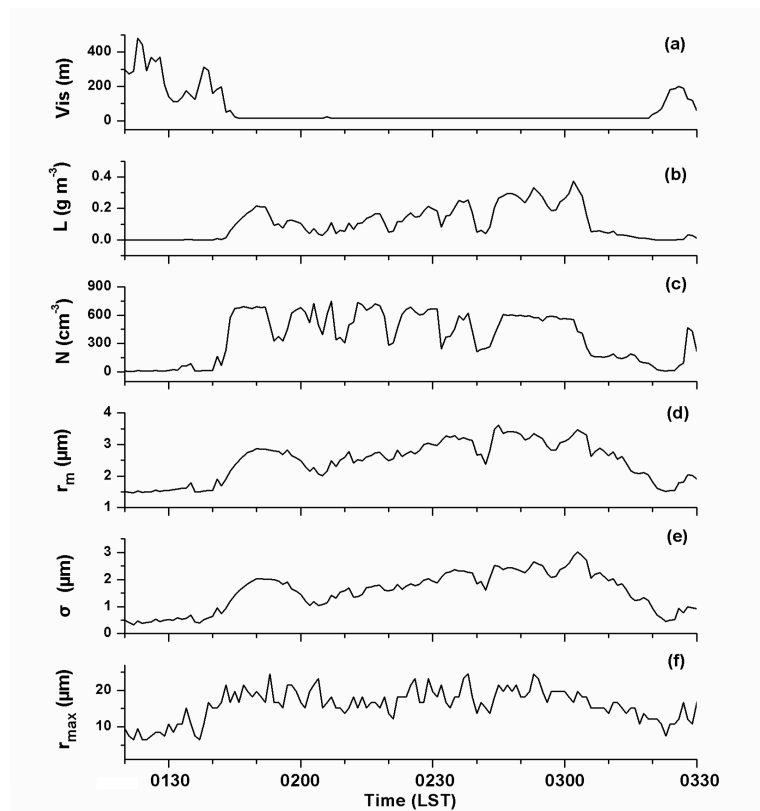


**Fig. 4** Temporal evolutions of (a) the visibility (*vis*), (b) the liquid water content (LWC), (c) the number concentration (*N*), (d) the mean radius (*r<sub>m</sub>*), (e) spectral standard deviation (*σ*), and (f) the maximum radius (*r<sub>max</sub>*) during 0120-0330 LST in the case 6.

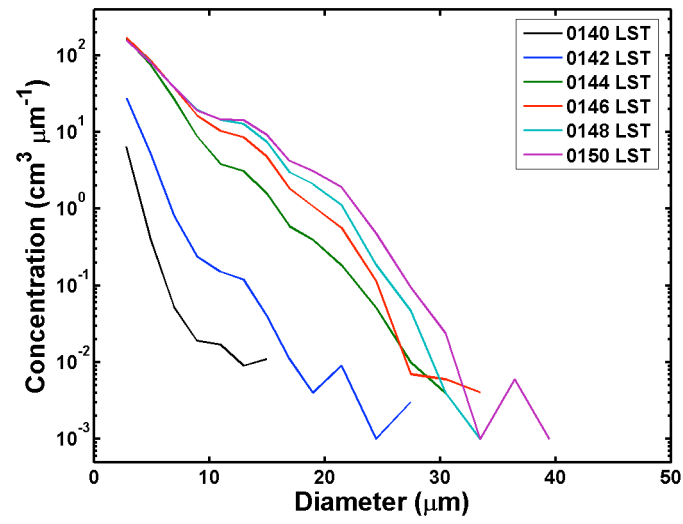


**Fig. 5** One minute average size distributions during the fog explosive development in the case 6.

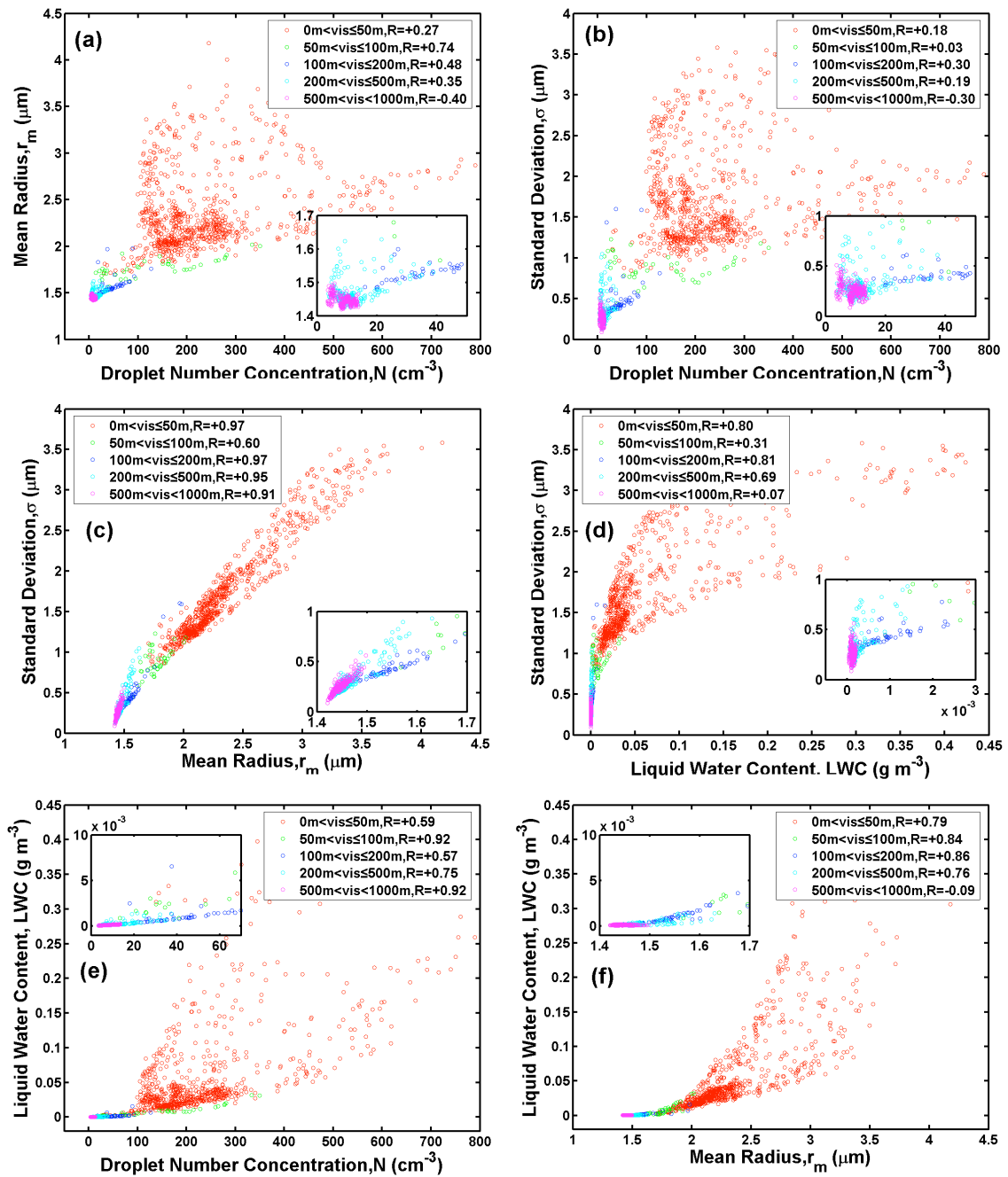


**Fig. 6** Relationships (a) between the mean radius ( $r_m$ ) and the droplet number concentration ( $N$ ), (b) between the standard deviation ( $\sigma$ ) and  $N$ , (c) between  $\sigma$  and  $r_m$ , (d) between the  $\sigma$  and the LWC, (e) between the LWC and the  $N$ , (f) between the LWC and the  $r_m$  for five visibility (vis) ranges in the case 6. The enlarged figures are added.

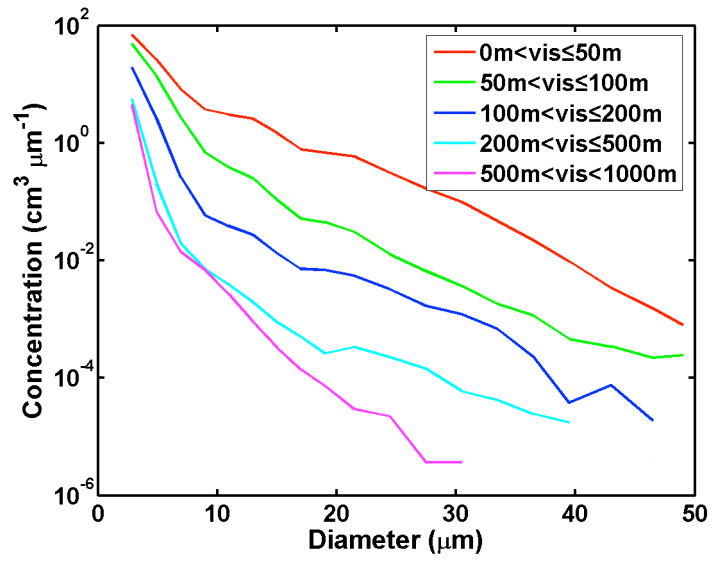


**Fig. 7** The average size distributions for different visibility (vis) ranges in the case 6.

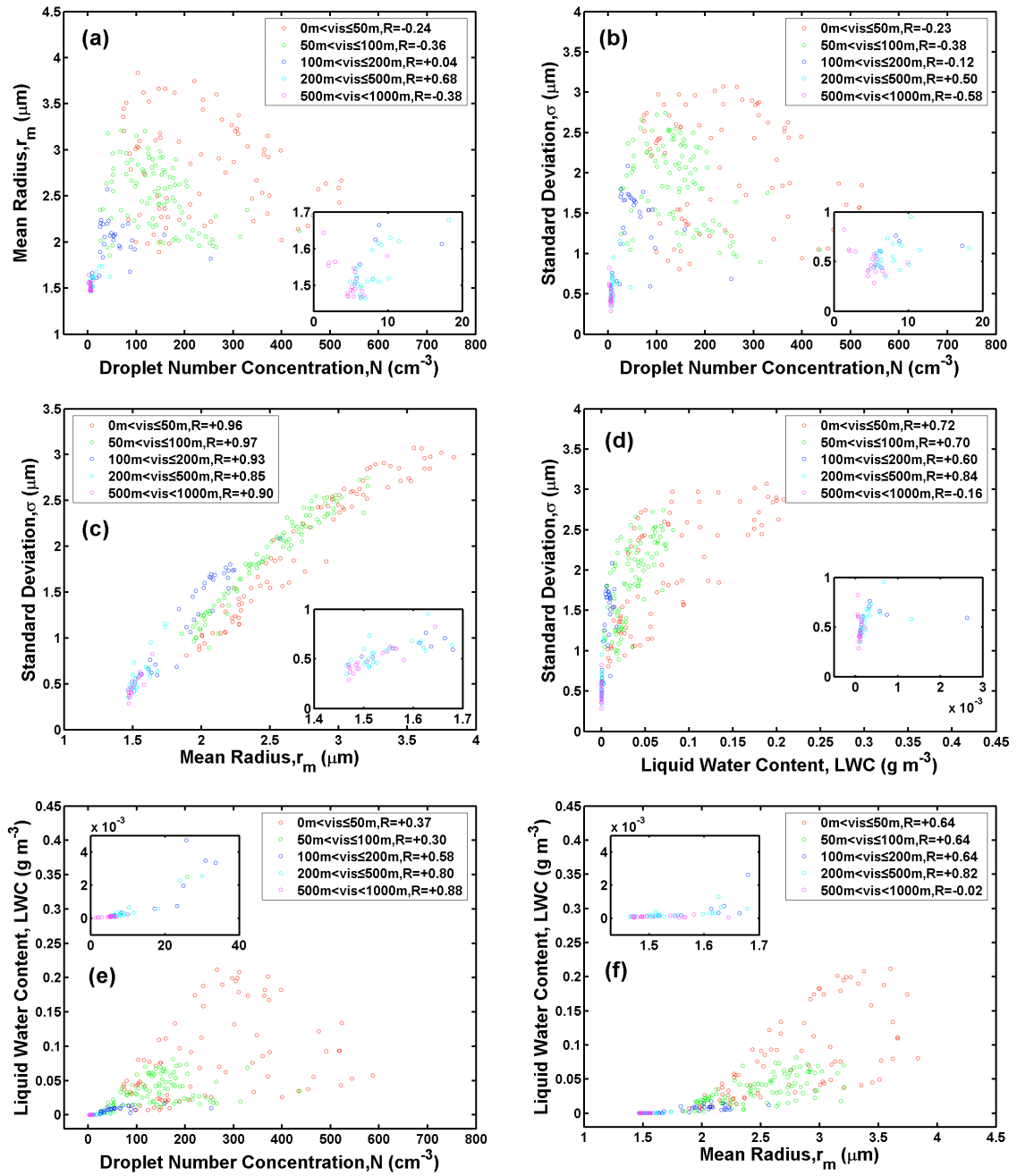
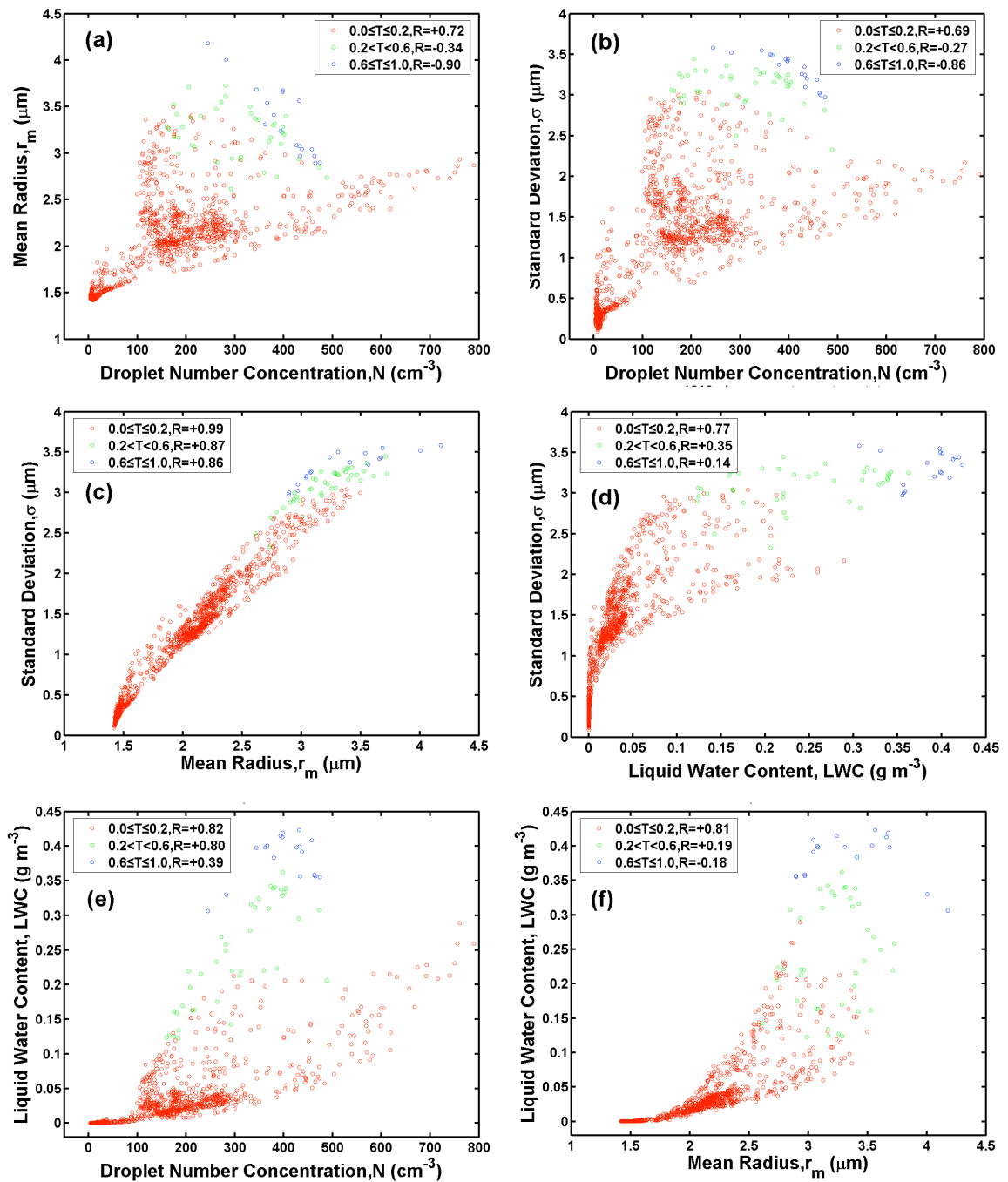


Fig.8 Same as Fig. 6 but for the case 8.



**Fig. 9** Relationships (a) between the mean radius ( $r_m$ ) and the droplet number concentration ( $N$ ), (b) between the standard deviation ( $\sigma$ ) and  $N$ , (c) between  $\sigma$  and  $r_m$ , (d) between the  $\sigma$  and the LWC, (e) between the LWC and the  $N$ , (f) between the LWC and the  $r_m$  for three autoconversion threshold function ( $T$ ) ranges in the case 6.